Schottky Barrier Rectifier Based on (100) β-Ga_2O_3 and its DC and AC Characteristics

Qiming He, Wenxiang Mu, Bo Fu, Zhitai Jia, Shibing Long, *Member, IEEE*, Zhaoan Yu, Zhihong Yao, Wei Wang, Hang Dong, Yuan Qin, Guangzhong Jian, Ying Zhang, Huiwen Xue, Hangbing Lv, *Member, IEEE*, Qi Liu, *Member, IEEE*, Minghua Tang, Xutang Tao, and Ming Liu, *Fellow, IEEE*

***Abstract*— A Schottky barrier rectifier was fabricated with a (100)-oriented β-Ga_2O_3 substrate grown by the edge-defined film-fed method. The Sn-doped β-Ga_2O_3 substrate had an effective donor concentration of approximately 2×10^{17} cm^{-3}. High performance parameters were obtained, such as a high forward current (421 A/cm^2 at 2 V), low ON-resistance (2.9 m$\Omega\cdot$cm^2), and short reverse recovery time (20 ns). Furthermore, the dynamic behavior of the device is characterized through test on the half-wave rectification of ac voltages at different frequency. The diode worked well at 100 kHz. At the end of the letter, we discuss how Ga_2O_3 Schottky rectifier can operate at high frequency.**

***Index Terms*—(100) β-Ga_2O_3, Schottky barrier rectifier, rectification characteristics.**

Manuscript received January 25, 2018; revised February 25, 2018; accepted February 26, 2018. Date of publication March 1, 2018; date of current version March 22, 2018. This work was supported in part by the National Natural Science Foundation of China under Grant 61521064, Grant 51472210, Grant 61322408, Grant 61422407, Grant 61522408, Grant 61574169, Grant 61334007, Grant 61474136, Grant 61574166, and Grant 61376112, in part by the Ministry of Science and Technology of China under Grant 2016YFA0201803, Grant 2016YFA0203800, and Grant 2017YFB0405603, in part by the Key Research Program of Frontier Sciences of the Chinese Academy of Sciences under Grant QYZDB-SSW-JSC048 and Grant QYZDY-SSW-JSC001, in part by the Beijing Municipal Science and Technology Project under Grant Z171100002017011, and in part by the Opening Project of the Key Laboratory of Microelectronics Devices and Integration Technology, Institute of Microelectronics, Chinese Academy of Sciences. The work of Z. Jia was supported in part by the Young Scholars Program of Shandong University under Grant 2015WLJH36 and in part by the State Key Laboratory of Optoelectronic Materials and Technologies, Sun Yat-sen University. The review of this letter was arranged by Editor D. G. Senesky. *(Qiming He and Wenxiang Mu contributed equally to this work.) (Corresponding author: Ming Liu.)*

Q. He is with the Key Laboratory of Key Film Materials and Application for Equipments (Hunan Province), School of Material Sciences and Engineering, Xiangtan University, Xiangtan 411105, China, also with the Key Laboratory of Microelectronics Devices and Integration Technology, Institute of Microelectronics, Chinese Academy of Sciences, Beijing 100029, China, also with the University of Chinese Academy of Sciences, Beijing 100049, China, and also with the Jiangsu National Synergetic Innovation Center for Advanced Materials, Nanjing 210023, China.

W. Mu, B. Fu, and X. Tao are with the State Key Laboratory of Crystal Materials and the Key Laboratory of Functional Crystal Materials and Device, Shandong University, Jinan 250100, China (e-mail: txt@sdu.edu.cn).

Z. Jia is with the State Key Laboratory of Crystal Materials and the Key Laboratory of Functional Crystal Materials and Device, Shandong University, Jinan 250100, China, and also with the State Key Laboratory of Optoelectronic Materials and Technologies, Sun Yat-sen University, Guangzhou 510275, China.

S. Long, Z. Yu, Z. Yao, W. Wang, H. Dong, Y. Qin, G. Jian, Y. Zhang, H. Xue, H. Lv, Q. Liu, and M. Liu are with the Key Laboratory of Microelectronics Devices and Integration Technology, Institute of Microelectronics, Chinese Academy of Sciences, Beijing 100029, China, also with the University of Chinese Academy of Sciences, Beijing 100049, China, and also with the Jiangsu National Synergetic Innovation Center for Advanced Materials, Nanjing 210023, China (e-mail: longshibing@ime.ac.cn; liuming@ime.ac.cn).

M. Tang is with the Key Laboratory of Key Film Materials and Application for Equipments (Hunan Province), School of Material Sciences and Engineering, Xiangtan University, Xiangtan 411105, China.

Color versions of one or more of the figures in this letter are available online at http://ieeexplore.ieee.org.

Digital Object Identifier 10.1109/LED.2018.2810858

I. Introduction

Currently, the rapid development of power electronics is promoting wide-bandgap semiconductor materials to apply into high power devices [1]–[4]. The rapid development of ultra-wide-bandgap β-Ga_2O_3 semiconductor is attracting focused interest [5]. β-Ga_2O_3 has advantages in unipolar devices comparing with SiC and GaN due to its more desirable material properties [6]. For instance, these semiconductors have an extremely large bandgap (E_g) of 4.5 - 4.9 eV [7]–[9]. Their breakdown electric field strength (E_b) is estimated to be as high as 6 - 8 MV/cm [10]. The Baliga's figure-of-merit (BFOM $= \varepsilon\mu E_b^3$, where ε is a relative dielectric constant and μ is electron mobility), which is the parameter used to evaluate the appropriateness of a material for a power device [1], of ultra-wide-bandgap β-Ga_2O_3 is four times larger than that of SiC and GaN [11]–[13]. The conventional low-cost melt methods, such as Czochralski, floating zone (FZ) and edge-defined film-fed growth (EFG), can be used to grow large high-quality single-crystal β-Ga_2O_3 wafers [10], [14]–[16], significantly reducing the cost of device production. Notably, many studies on β-Ga_2O_3 Schottky barrier diodes (SBDs), which constitute very important discrete and integral power devices, have been reported [17]–[23]. In these studies, the device structures are usually simple, but the device performance is adequate with respect to forward current, ON-resistance, and reverse breakdown voltage based on DC electrical measurements. However, the dynamic behavior of Ga_2O_3 SBDs (especially the rectifying modulation on the AC signal) has not been investigated in depth. The dynamic behavior of the diode is commonly evaluated for switching operations induced by rectification in an AC-DC converter circuit [24]. Furthermore, the β-Ga_2O_3 crystals used in SBD typically have (001), ($\bar{2}$01) and (001) orientations [17]–[22], but the (100)-oriented crystal is rarely used in SBD. In our previous work [23], we fabricated and characterized a simple SBD with (100) β-Ga_2O_3 that shows acceptable device performance.

0741-3106 © 2018 IEEE. Translations and content mining are permitted for academic research only. Personal use is also permitted, but republication/redistribution requires IEEE permission. See http://www.ieee.org/publications_standards/publications/rights/index.html for more information.

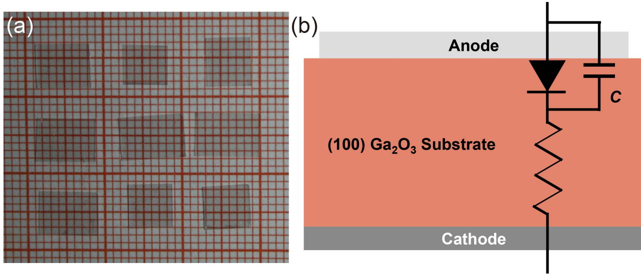

Fig. 1. (a) (100)-oriented β-Ga_2O_3 substrates used for Schottky barrier diode (SBD) fabrication. (b) Schematic structure and equivalent circuit [24], [25] of the Pt/(100)β-Ga_2O_3 SBD.

In this work, we optimized crystal growth parameters and improved the Sn doping concentration. The new device shows markedly improved performance, including forward current density ($J_{@2V}$), ON-state resistance (R_{ON}), and a reverse breakdown property, and the rectification ability for AC signals under different frequencies was also demonstrated.

II. Experiments

The (100)-oriented β-Ga_2O_3 substrates grown by the EFG method [14] are rectangular blocks smaller than 10 mm $\times$ 10 mm with thickness of about 480 nm, as shown in Fig. 1(a). The quality of the crystal was also improved in this work by optimizing the thermal field and seeding process during the growth [14]. SnO_2 powder was intentionally added into the raw material, which makes the n-type carrier concentration reaches 2×10^{17} cm^{-3}, as obtained by the Hall test and capacitance voltage ($C - V$) test. A high surface quality with root-mean-square (RMS) roughness of about 0.1 nm was obtained after mechanical exfoliation [16]. The schematic structure of the Schottky barrier diode is shown in Fig. 1(b), which is composed of a Pt/β-Ga_2O_3 Schottky contact and a Ti/β-Ga_2O_3 Ohmic contact. The fabrication method of this device is similar to that in our previous work [23]. The Au (40 nm)/Ti (10 nm)/Pt (30 nm) anode and Ti (20 nm)/Au (40 nm) cathode metal films were both deposited by magnetron sputtering. The 400 ° oxygen plasma treatment were applied prior to sputtering cathode to optimize ohmic contact. The circular Schottky electrodes have a diameter of 150 μm. The current density-voltage ($J - V$) and C–V curves were measured by a semiconductor device analyzer (Agilent B1500A, Agilent Technologies, Santa Clara, CA, USA) and a semiconductor characterization system (Keithley 4200A-SCS, Tektronix Inc., Beaverton, OR, USA). A pulse generator unit (Agilent B1530A, Agilent Technologies, Santa Clara, CA, USA) was used to test the reverse recovery time of the SBD. A rectification circuit was configured (Fig. 4(a)), and by applying AC signals generated by an arbitrary function generator (AFG3102, Tektronix Inc., Beaverton, OR, USA), the waveforms during the rectification process were monitored by an oscilloscope (MSO9404A, Agilent Technologies, Santa Clara, CA, USA).

III. Results and Discussion

We first characterized the DC $J - V$ and AC C–V curves of the Pt/(100)β-Ga_2O_3/Ti SBD. Fig. 2(a) shows the semi-log and linear forward $J - V$ characteristics of the SBD measured at room temperature (RT). For comparison, the curve obtained

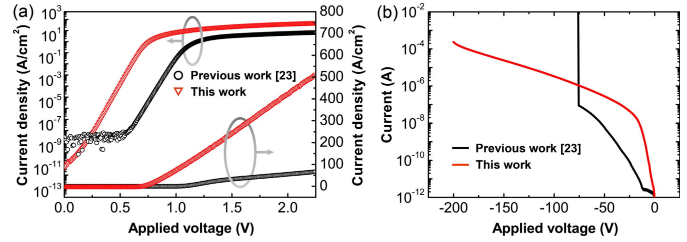

Fig. 2. (a) Liner and semi-logarithmic plot of the forward $J - V$ curve of the Pt/(100)β-Ga_2O_3 SBD in this work (red lines) and in our previous work (black lines) [23]. (b) Reverse $I - V$ curve of Pt/(100)β-Ga_2O_3 SBD compared with previous work [23].

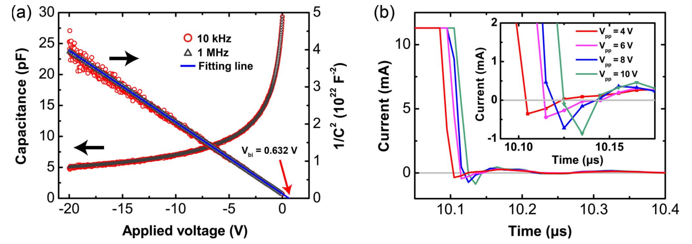

Fig. 3. (a) $C - V$ and $1/C^2 - V$ characteristics of the SBD measured at 10 kHz (red circles) and 1 MHz (gray triangles). The blue straight line is the fitting result. (b) Reverse recovery time of the SBD measured under V_{pp} from 4 V to 10 V.

in our previous work is also plotted in this figure. The device shows a high forward current density, reaching 421 A/cm^2 at the applied voltage of 2 V ($J_{@2V}$), which is 7 times that in our previous work [23]. The ON-state resistance (R_{ON}) was significantly reduced to 2.9 mΩ·cm^2, much lower than the value of 12.5 mΩ·cm^2 reported in our previous work [23]. Fig. 2(b) shows the reverse $I - V$ characteristics of the Ga_2O_3 SBD. The device still does not breakdown under a 200 V reverse bias voltage. Due to the limitations of the instrument and probe station, we cannot further strengthen the voltage. However, from the current value (2.3×10^{-4} A at 200 V), we can estimate that the breakdown voltage is larger than this test value. The leakage current is larger than that in our previous work [23], mainly caused by the lower barrier height that is influenced by the higher doping concentration of the wafer [26]. Device structures with epi-layer [19], [21], field plate [20], field ring [27], and trench [22] are good ways to solve this problem.

Fig. 3(a) shows the C–V and $1/C^2 - V$ plot for the SBD at 10 kHz and 1 MHz at RT. The linear relationship between $1/C^2$ and V indicates the uniform doping of the substrate, and the difference between the two lines appears to be very slight, showing that few deep level impurities exist in the Ga_2O_3 semiconductor [28]. From the linear fitting results, the value of the threshold voltage or built-in potential (V_{bi}) is 0.63 V, lower than the value of 1.07 V in the literature [23], mainly due to the increased carrier concentration.

A diode is usually a rectifier in a circuit and must work at different frequencies. To investigate whether our diode has rectification ability when working at high frequency, we first tested the reverse recovery time (RRT) of the SBD, with the testing result shown in Fig. 3(b). The diode was switched with the applied bias voltage abruptly decreasing from forward to reverse with peak to peak value (V_{pp}) from 4 V to 10 V. The result shows that the RRT is approximately 20 ns, which

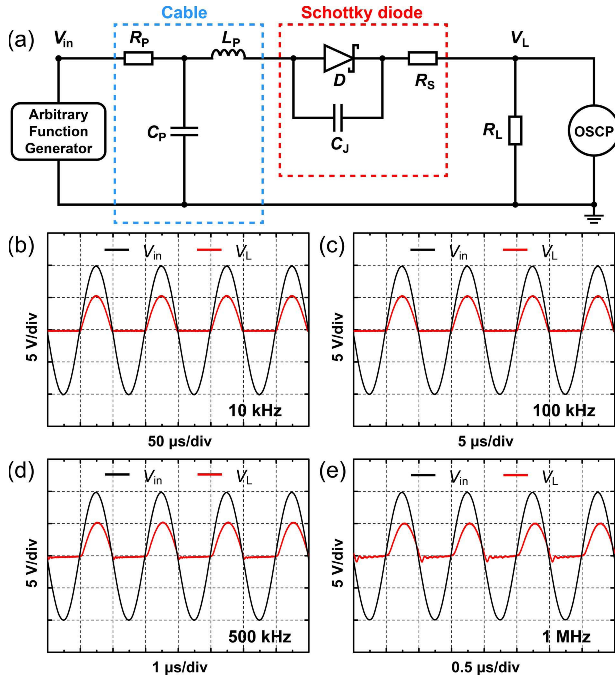

Fig. 4. (a) Rectification circuit. Rectification characteristics of the SBD measured under (b) f =10 kHz, (c) f = 100 kHz, (d) f = 500 kHz, and (e) f = 1 MHz. The load resistance R_L = 100 Ω. C_P, R_P and L_P are the parasitic capacitance, resistance and inductance from the cable, respectively.

is a very short time and does not change with increasing amplitude of the signal, indicating that the fabricated SBD has the potential to switch at high frequency.

Next, we tested the rectification characteristics of the diode under the AC frequency ≥ 10 kHz. First, we built a simple rectifier and filter circuit, as shown in Fig. 4(a). The circuit consists of a Pt/(100)β-Ga_2O_3 rectifying diode (D), including its junction capacitance (C_J) and series resistance (R_S), framed in the red dotted box, in series with a load resistance (R_L) representing the load of the eventual circuit. The parasitic effects from the probe station were almost completely eliminated, by disconnecting its chuck. On the other hand, the parasitic effects from the cable can also be obviously weakened by shortening its length, and its remnant parasitic effects especially under high frequency can be described by using the transmission line model, as shown in the blue dotted box in Fig. 4(a). R_P, L_P, and C_P are the parasitic resistance, inductance and capacitance in the testing circuit, respectively.

The input AC signal with 20 V peak-peak value was generated by the signal generator, and the input (V_{in}) and output (V_L) waveforms were measured by the oscilloscope. The black curves in Figs. 4(b) to 4(e) are the original sine waveform input signals V_{in} under different frequency f, and the red curves show the output signal V_L. Half sine waveforms of the output V_L similar to that of the input V_{in} are presented, which is just led by the rectifying effect of the rectifier. From Figs. 4(b) to 4(e), we can also see that the amplitudes of V_L keep constant under different frequencies and are just half those of V_{in}, which is determined by that the value of R_L was kept constant and just equivalent to that of the cable and R_L. The slight phase delay of the output waveform when the rectifier operates over 500 kHz is caused by the inductance in the cable. In general, Fig. 4 shows that the diode still does not lose the rectification capability even in a frequency of 1 MHz. However, we can see a small amount of negative current in Fig. 4(e). This phenomenon is originated from the more and more obvious reverse recovery characteristic of our device under higher frequency that is influenced by the junction capacitance.

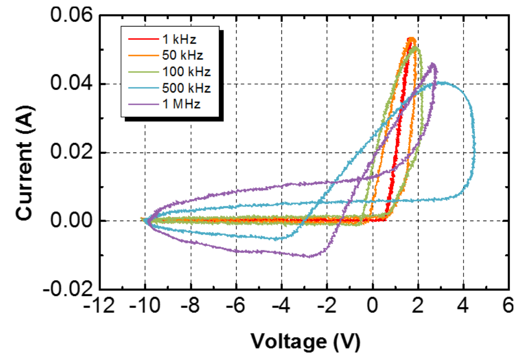

Fig. 5. Lissajous plot as $I-V$ characteristics for rectification operation of the SBD form 1 kHz to 1 MHz.

Fig. 5 shows the I–V characteristics of the SBD as a Lissajous curve of the applied AC frequency. Lissajous parttern is a method for analyzing residual charges in diodes [24]. It shows that the I–V characteristics of the SBD are ideal when operating at a frequency of up to 100 kHz.

All these results indicate that the rectifier based on (100) β-Ga_2O_3 has the ideal rectification ability working under 100 kHz. To investigate the possiblity of improving operation frequency, let's anlyze the possible role of the barrier capacitance (C_J) of our SBD through its equivalent circuit as shown in both Fig. 1(b) and Fig. 4(a). As C_J is in parallel with the Schottky junction, its impedance $(\omega C_J)^{-1}$, reduces with increasing frequency. Thus in high frequency, the Schottky junction will be shorted, resulting in the reduction or even loss of the rectification capacity. Therefore, for high frequency operation and application, low junction capacitance of the device is needed, which can be achieved by introducing epitaxy layer with low doping concentration or using ultrathin wafer with low doping concentration.

IV. Conclusion

In this study, a Schottky rectifier was fabricated with a (100) β-Ga_2O_3 single-crystal substrate with a comparatively high doping concentration. The device, which has a simple structure, shows good forward electrical characteristics, such as low on-resistance (R_{on}), low threshold voltage (V_{bi}), high on-state current density (J_{on}), which are good enough compared to other works on Ga_2O_3 [17]–[22], SiC [29]–[31] and GaN [32]–[34]. Our device also shows good reverse electrical characteristics, including a very short reverse recovery time comparable to the reported value [21], and a breakdown voltage of about 200 V which is higher than that of other Ga_2O_3 wafer based devices [17]. The dynamic behavior was tested by using a half-wave rectification circuit. The result indicates that the device has the ideal working frequency of 100 kHz, which is equivalent to that of SiC [24]. These results indicate that Ga_2O_3 semiconductor has a good potential for power device application.

REFERENCES

[1] B. J. Baliga, *Fundamentals of Power Semiconductor Devices*. Springer, 2010, pp. 23–55.

[2] T. P. Chow and R. Tyagi, "Wide bandgap compound semiconductors for superior high-voltage unipolar power devices," *IEEE Trans. Electron Devices*, vol. 41, no. 8, pp. 1481–1483, Aug. 1994, doi: 10.1109/16.297751.

[3] J. Millan, P. Godignon, X. Perpina, A. Perez-Tomas, and J. Rebollo, "A survey of wide bandgap power semiconductor devices," *IEEE Trans. Power Electron.*, vol. 29, no. 5, pp. 2155–2163, May 2014, doi: 10.1109/TPEL.2013.2268900.

[4] T. P. Chow, I. Omura, M. Higashiwaki, H. Kawarada, and V. Pala, "Smart power devices and ICs using GaAs and wide and extreme bandgap semiconductors," *IEEE Trans. Electron Devices*, vol. 64, no. 3, pp. 856–873, Mar. 2017, doi: 10.1109/TED.2017.2653759.

[5] S. J. Pearton, J. Yang, P. H. Cary, IV, F. Ren, J. Kim, M. J. Tadjer, and M. A. Mastro, "A review of Ga_2O_3 materials, processing, and devices," *Appl. Phys. Rev.*, vol. 5, no. 1, p. 011301, Jan. 2018, doi: 10.1063/1.5006941.

[6] M. Higashiwaki, A. Kuramata, H. Murakami, and Y. Kumagai, "State-of-the-art technologies of gallium oxide power devices," *J. Phys. D, Appl. Phys.*, vol. 50, no. 33, p. 333002, Jul. 2017, doi: 10.1088/1361-6463/aa7aff.

[7] M. Orita, H. Ohta, M. Hirano, and H. Hosono, "Deep-ultraviolet transparent conductive β-Ga_2O_3 thin films," *Appl. Phys. Lett.*, vol. 77, no. 25, pp. 4166–4168, Dec. 2000, doi: 10.1063/1.1330559.

[8] H. H. Tippins, "Optical absorption and photoconductivity in the band edge of β-Ga_2O_3," *Phys. Rev.*, vol. 140, no. 1a, pp. A316–A319, Oct. 1965, doi: 10.1103/PhysRev.140.A316.

[9] H. He, R. Orlando, M. A. Blanco, R. Pandey, E. Amzallag, I. Baraille, and M. Rérat, "First-principles study of the structural, electronic, and optical properties of Ga_2O_3 in its monoclinic and hexagonal phases," *Phys. Rev. B, Condens. Matter*, vol. 74, no. 19, p. 195123, Nov. 2006, doi: 10.1103/PhysRevB.74.195123.

[10] N. Ueda, H. Hosono, R. Waseda, and H. Kawazoe, "Synthesis and control of conductivity of ultraviolet transmitting β-Ga_2O_3 single crystals," *Appl. Phys. Lett.*, vol. 70, no. 26, pp. 3561–3563, Nov. 1997, doi: 10.1063/1.119233.

[11] M. Higashiwaki, K. Sasaki, A. Kuramata, T. Masui, and S. Yamakoshi, "Development of gallium oxide power devices," *Phys. Status Solidi A*, vol. 211, no. 1, pp. 21–26, Nov. 2014, doi: 10.1002/pssa.201330197.

[12] M. Higashiwaki, K. Sasaki, H. Murakami, Y. Kumagai, A. Koukitu, A. Kuramata, T. Masui, and S. Yamakoshi, "Recent progress in Ga_2O_3 power devices," *Semicond. Sci. Technol.*, vol. 31, no. 3, p. 034001, Jan. 2016, doi: 10.1088/0268-1242/31/3/034001.

[13] S. Fujita, "Wide-bandgap semiconductor materials: For their full bloom," *Jpn. J. Appl. Phys.*, vol. 54, no. 3, p. 030101, 2015, doi: 10.7567/JJAP.54.030101.

[14] W. Mu, Z. Jia, Y. Yin, Q. Hu, Y. Li, B. Wu, J. Zhang, and X. Tao, "High quality crystal growth and anisotropic physical characterization of β-Ga_2O_3 single crystals grown by EFG method," *J. Alloys Compounds*, vol. 714, pp. 453–458, Apr. 2017, doi: 10.1016/j.jallcom.2017.04.185.

[15] Y. Tomm, P. Reiche, D. Klimm, and T. Fukuda, "Czochralski grown Ga_2O_3 crystals," *J. Cryst. Growth*, vol. 220, no. 4, pp. 510–514, Dec. 2000, doi: 10.1016/S0022-0248(00)00851-4.

[16] W. Mu, Z. Jia, Y. Yin, Q. Hu, J. Zhang, Q. Feng, Y. Hao, and X. Tao, "One-step exfoliation of ultra-smooth β-Ga_2O_3 wafers from bulk crystal for photodetectors," *CrystEngComm*, vol. 19, no. 34, pp. 5122–5127, Aug. 2017, doi: 10.1039/C7CE01076A.

[17] K. Sasaki, M. Higashiwaki, A. Kuramata, T. Masui, and S. Yamakoshi, "Ga_2O_3 Schottky barrier diodes fabricated by using single-crystal β-Ga_2O_3 (010) substrates," *IEEE Electron Device Lett.*, vol. 34, no. 4, pp. 493–495, Mar. 2013, doi: 10.1109/LED.2013.2244057.

[18] O. Toshiyuki, K. Yuta, H. Kazuya, and K. Makoto, "High-mobility β-$Ga_2O_3(\bar{2}01)$ single crystals grown by edge-defined film-fed growth method and their Schottky barrier diodes with Ni contact," *Appl. Phys. Exp.*, vol. 8, no. 3, p. 031101, Feb. 2015, doi: 10.7567/APEX.8.031101.

[19] M. Higashiwaki, K. Konishi, K. Sasaki, K. Goto, K. Nomura, Q. T. Thieu, R. Togashi, H. Murakami, Y. Kumagai, B. Monema, A. Koukitu, A. Kuramata, and S. Yamakoshi, "Temperature-dependent capacitance–voltage and current–voltage characteristics of Pt/Ga_2O_3 (001) Schottky barrier diodes fabricated on n^--Ga_2O_3 drift layers grown by halide vapor phase epitaxy," *Appl. Phys. Lett.*, vol. 108, no. 13, p. 133503, Mar. 2016, doi: 10.1063/1.4945267.

[20] K. Konishi, K. Goto, H. Murakami, Y. Kumagai, A. Kuramata, S. Yamakoshi, and M. Higashiwaki, "1-kV vertical Ga_2O_3 field-plated Schottky barrier diodes," *Appl. Phys. Lett.*, vol. 110, no. 10, p. 103506, Feb. 2017, doi: 10.1063/1.4977857.

[21] J. Yang, S. Ahn, F. Ren, S. J. Pearton, S. Jang, J. Kim, and A. Kuramata, "High reverse breakdown voltage Schottky rectifiers without edge termination on Ga_2O_3," *Appl. Phys. Lett.*, vol. 110, no. 19, p. 192101, Apr. 2017, doi: 10.1063/1.4983203.

[22] K. Sasaki, D. Wakimoto, Q. T. Thieu, Y. Koishikawa, A. Kuramata, M. Higashiwaki, and S. Yamakoshi, "First demonstration of Ga_2O_3 trench MOS-type Schottky barrier diodes," *IEEE Electron Device Lett.*, vol. 38, no. 6, pp. 783–785, Jun. 2017, doi: 10.1109/LED.2017.2696986.

[23] Q. He, W. Mu, H. Dong, S. Long, Z. Jia, H. Lv, Q. Liu, M. Tang, X. Tao, and M. Liu, "Schottky barrier diode based on β-Ga_2O_3 (100) single crystal substrate and its temperature-dependent electrical characteristics," *Appl. Phys. Lett.*, vol. 110, no. 9, p. 093503, Feb. 2017, doi: 10.1063/1.4977766.

[24] T. Funaki, T. Kimoto, and T. Hikihara, "Evaluation of high frequency switching capability of SiC Schottky barrier diode, based on junction capacitance model," *IEEE Trans. Power Electron.*, vol. 23, no. 5, pp. 2602–2611, Sep. 2008, doi: 10.1109/TPEL.2008.2002096.

[25] M. K. Kazimierczuk, *Pulse-Width Modulated DC-DC Power Converters*. Hoboken, NJ, USA: Wiley, 2015, p. 810.

[26] J. M. Shannon, "Control of Schottky barrier height using highly doped surface layers," *Solid-State Electron.*, vol. 19, no. 6, pp. 537–543, Jun. 1976, doi: 10.1016/0038-1101(76)90019-8.

[27] K. Ueno, T. Urushidani, K. Hashimoto, and Y. Seki, "The guard-ring termination for the high-voltage SiC Schottky barrier diodes," *IEEE Electron Device Lett.*, vol. 16, no. 7, pp. 331–332, Jul. 1995, doi: 10.1109/55.388724.

[28] S. M. Sze, and K. K. Ng, *Physics of Semiconductor Devices*. Hoboken, NJ, USA: Wiley, 2006, pp. 138–139.

[29] V. Khemka, V. Ananthan, and T. P. Chow, "A fully planarized 4H-SiC trench MOS barrier Schottky (TMBS) rectifier," *IEEE Electron Device Lett.*, vol. 21, no. 6, pp. 286–288, Jun. 2000, doi: 10.1109/55.843152.

[30] J. H. Zhao, P. Alexandrov, and X. Li, "Demonstration of the first 10-kV 4H-SiC Schottky barrier diodes," *IEEE Electron Device Lett.*, vol. 24, no. 6, pp. 402–404, Jun. 2003, doi: 10.1109/LED.2003.813370.

[31] T. Nakamura, T. Miyanagi, I. Kamata, T. Jikimoto, and H. Tsuchida, "A 4.15 kV 9.07-mΩ.cm^2 4H-SiC Schottky-barrier diode using Mo contact annealed at high temperature," *IEEE Electron Device Lett.*, vol. 26, no. 2, pp. 99–101, Feb. 2005, doi: 10.1109/LED.2004.841473.

[32] M. Zhu, B. Song, M. Qi, Z. Hu, K. Nomoto, X. Yan, Y. Cao, W. Johnson, E. Kohn, D. Jena, and H. G. Xing, "1.9-kV AlGaN/GaN lateral Schottky barrier diodes on silicon," *IEEE Electron Device Lett.*, vol. 36, no. 4, pp. 375–377, Apr. 2015, doi: 10.1109/LED.2015.2404309.

[33] Q. Zhou, Y. Jin, Y. Shi, J. Mou, X. Bao, B. Chen, and B. Zhang, "High reverse blocking and low onset voltage AlGaN/GaN-on-Si lateral power diode with MIS-gated hybrid anode," *IEEE Electron Device Lett.*, vol. 36, no. 7, pp. 660–662, Jul. 2015, doi: 10.1109/LED.2015.2432171.

[34] Y. Zhang, M. Sun, Z. Liu, D. Piedra, M. Pan, X. Gao, Y. Lin, A. Zubair, L. Yu, and T. Palacios, "Novel GaN trench MIS barrier Schottky rectifiers with implanted field rings," in *IEDM Tech. Dig.*, San Francisco, CA, USA, Dec. 2016, pp. 10.2.1–10.2.4, doi: 10.1109/IEDM.2016.7838386.